Published by Avanti Publishers

Journal of Advances in Applied & Computational Mathematics

ISSN (online): 2409-5761

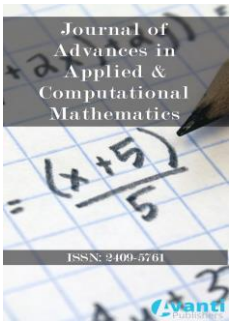

Biomagnetic Fluid Flow on a Nonlinearly Stretching Sheet with Variable Thickness in a Magnetic Environment

Md. Ghulam Murtaza[1], Jagadis C. Misra[2], Efstratios E. Tzirtzilakis[3] and Mohammad Ferdows[4]

[1]*Department of Mathematics, Comilla University, Cumilla 3506, Bangladesh*

[2]*Department of Mathematics, Ramakrishna Mission Vidyamandira (Autonomous Postgraduate College), Belur Math, Howrah-711202, India*

[3]*Fluid Mechanics and Turbomachinary Laboratory, Department of Mechanical Engineering, University of the Peloponnese, Tripoli, Greece*

[4]*Research Group of Fluid Flow Modeling and Simulation, Department of Applied Mathematics, University of Dhaka, Dhaka-100, Bangladesh*

ARTICLE INFO

Article Type: Research Article

Academic Editor: Fabio Gobbi

Keywords:
Ferrofluid
Magnetization
Stretching sheet
Biomagnetic fluid
Variable thickness

Timeline:
Received: November 10, 2023
Accepted: December 13, 2023
Published: December 29, 2023

Citation: Murtaza MG, Misra JC, Tzirtzilakis EE, Ferdows M. Biomagnetic fluid flow on a nonlinearly stretching sheet with variable thickness in a magnetic environment. J Adv App Comput Math. 2023; 10: 163-177.

DOI: https://doi.org/10.15377/2409-5761.2023.10.14

ABSTRACT

The main contribution of the current work is a numerical and mathematical investigation of the effects of magnetic dipole and electrical conductivity on the heat and flow transfer of biomagnetic fluid over a non-linear stretched sheet with variable thickness. Static magnetic fields are produced by magnetic dipoles, which are used in medical a pplications such as MRI, drug administration, and cancer therapy. Additionally, the impact of non-linear heat source/sink features was examined in the study, leading to an interesting phenomenon. The PDEs are attenuated to nonlinear ODEs with dealing appropriate similarity variables. These resultant ODEs are computed by developing an effective method emerged on the application of the finite differences technique. In the end, this section offers a summary of the implications resulting from different physical limitations on blood flow, including variable thickness and power index effects. It was discovered that the rise in Kelvin and Lorentz forces in the boundary layer significantly affected blood flow. The current findings for the biomagnetic fluid model are novel and inventive since they effectively expand upon the issues previously addressed by previously published scientific documentation.

*Corresponding Author
Email: ferdows@du.ac.bd
Tel: +(880) 1720809796

1. Introduction

Biological fluids present in living systems, whose flow is influenced by magnetic fields are usually referred to as biomagnetic fluids. Various investigations related to the dynamical behavior of biomagnetic fluids constitute a separate area of fluid dynamics, called biomagnetic fluid dynamics (BFD). Blood is a characteristic example of biomagnetic fluid. During the past few decades researchers have tried to explore various aspects of BFD by resorting to experimental/theoretical techniques. These studies [1-6] have enriched the fields of physiology, medicine and bioengineering. There are numerous application of biological fluids, among of them is cell separation, for therapy procedure such as electromagnetic hyperthermia used in the treatment of malignant tumors, magnetic therapy for wound healing and magnetic particle imagine (MPI), which is a novel imagine technique used in iron oxide nanoparticle tracers, anticancer treatment, reducing bleeding during surgeries and the development of medical device.

Under the purview of BFD, magnetic effect on the flow of a biological fluid is studied, by combining the principles of ferrohydrodynamics (FHD) and magnetohydrodynamics (MHD). This has been elaborated in the previous communications [4, 5] dealing with different features of biomagnetic flows of viscoelastic fluids. Misra *et al*. [6] discussed the blood flow analysis through arteries during cancer treatment by electromagnetic hyperthermia. Further discussion on biomagnetic fluid flow on stretching sheets are available in [7-10].

Generally, many biological processes are the potential to be affected by the use of external magnetic field. Characteristic biological flow via the human arterial way change under the influence of magnetic fields. The mathematical model of biological fluid was developed first by Jaik *et al*. [11]. This model follows to the knowledge of FHD [12-14]. These authors argue that for a fuller representation of blood flow, the performance of MHD force generated owing to electric field. Further, Tzirtzilakis [15] extended the BFD model, where he first included the Lorentz force. This model develop by considering both magnetization and polarization and he concluded that the magnetic field resist the flow field. Ramamurthy and Shanker [16] investigated the non-Newtonian blood flow using electromagnetic technique. A finite difference scheme with SIMPLE-type algorithm was used by Rusli *et al*. [17] to analysis the biomagnetic fluid mechanism. The governing equations, which are basically nonlinear PDEs are solved by using staggered grid. The study was conducted for channel flow that takes place subject to magnetic field whose strength varies spatially. The study exhibits that in the vicinity of the magnetic source, there is a possibility of vortex formation in the fluid mass. The extension of BFD model considering MHD and/or FHD was also found in [18-19] subject to external magnetic field.

Pavlov [20] examined the viscous flow of an MHD fluid by considering boundary layer approximation with magnetic field. Andersson [21-22], Lok *et al*. [23], Dulal *et al.* [24], Ishak *et al.* [25-27] performed different studies to examine the characteristics of various fluids flowing over stretching sheets under the influences of magnetic field. Anderson [28] discussed the flow field of MHD fluid subject to an extendable sheet, by considering the joint effects of fluid viscoelasticity and the presence of a magnetic field. This analysis shows that the effect of a magnetic field strength on the flow field is qualitatively similar to the effect of enhancing the fluid viscoelasticity. Mistikawy [29] examined MHD flow on a sheet that was stretching linearly while taking the produced magnetic field into account. Due to the appreciable performance on fluid heat transformation, Ali *et al*. [30-31] studied the MHD flow subject to extendable sheet. Different investigations on MHD flow with a variable temperature-dependent surface parameter and power law were presented in [32-33].

As though the majority of the researchers investigated at the BFD flow across a stretching sheet that was both linear and nonlinear and had a constant thickness. The flow analysis was first carried out across a stretching (non-linear) sheet with varying thickness by Fang *et al*. [34]. They found that variations in thickness cause boundary layer growth, which is similar to the results seen for a simple stretching sheet [34]. Subsequently, Lee [35] examined the flow analysis across a thin body with varying thickness. Many researchers have reported on the varied effects of controlling parameters on the flow field and heat transfer with variable-thickness stretching sheets, including Ishak *et al*. [36], Khader *et al*. [37], Prasad *et al*. [38], and Vajravelu *et al*. [39]. The MHD fluid flow exposed to stretching or

shrinking was investigated by Rashed *et al*. [40]. Based on theoretical results, they found that fluid heat flow was considerably increased by higher magnetic field parameter values, particularly in the stretching scenario when compared to the shrinking situation. Rashed *et al*. [41] examined a mathematical study of the one-parameter group technique, a group of transformation, to explain the effects of thermal and Brownian diffusion on nanofluid flow over a stretchable sheet. Using the shooting technique, they found that whenever nanoparticles combined with base fluid, the rate of heat transmission increased noticeably. Using group transformations, Rashed *et al*. [42] investigated the continuous nanofluid flow via cylindrical tubes. Because of their greater thermal conductivity, they discovered that silver nanoparticles produced the highest thermal values. Using a one-parameter group transformation technique, Rashed *et al*. [43] explored the significance of thermal radiation on MHD fluid past a moving heated plate. In order to separate free water from soil in an oil field with coalescing plates, Qi *et al*. [44] looked into flow field properties. Wang *et al*. [45] looked into the effects of flow field and electric field coupling on oil-water emulsion separation. Following twenty minutes of application of a square-wave electric field operating at a frequency of 3 kHz and an intensity of 2.0 kV/cm, they observed that the emulsified water separation rate exceeded 90% and the water content at the oil outflow was less than 1.5%.

Considering the importance of biomagnetic fluid flow problem in biomedical engineering systems and the state of the art of related studies, the current study's novel features include the following:

(i) The mechanical behavior of a biomagnetic fluid with a variable thickness property that passed through a stretchable sheet at a nonlinear velocity.

(ii) To take into account the magnetization and electrical conductivity caused by the blood's magnetic quality.

(iii) To take blood pressure into account.

(iv) To take the heat source/sink's impact into account.

(v) Developed the finite difference approach, a novel computer methodology, to address the given mathematical problem.

(vi) In this simulation, the combined effects of the variable thickness, magnetic field, and ferromagnetic interaction parameters are ameliorated.

(vii) Showing the variations of blood velocity, temperature, pressure profiles along with physical quantities such as skin friction coefficient, wall pressure gradient and the rate of heat transfer under the potential ranges of physical parameters.

According to the authors' best knowledge, these mathematical presumptions were not made before looking into the BFD difficulties. We believed that this research would contribute to our understanding of the basic mechanisms underlying blood properties and offer important information that could potentially save lives.

2. Basic Equations of the Mathematical Problem

We take into consideration that the current problem is two-dimensional, and involves a viscous, incompressible biomagnetic fluid across a non-linear stretching sheet of varying thickness which moves with velocity $\mathrm{u(x,y)} = \mathrm{U_w} = \mathrm{U_0(x+b)^m}$, along x axis where U_0 and b are constant as seen in Fig. (**1**). Also considered that at $y \geq 0$, the fluid flow is taken; where y is the vertical coordinate which is the normal to the sheet. Further, we assume that the model must be satisfied only for thickness sheet (not flat), where the thickness is defined by $A(x+b)^{\frac{1-m}{2}}$, here $\mathrm{A}$and m are constant. Since we intend to deal with a sheet which is not flat, we consider $\mathrm{m} \neq 1$. T_w is the sheet temperature, while ambient blood temperature is $\mathrm{T_c}$ such that $\mathrm{T_c} > \mathrm{T_w}$. The magnetic dipole, whose existence produces the strength of the magnetic field, is intended to be positioned at a distance$\mathrm{d}$ below the sheet.

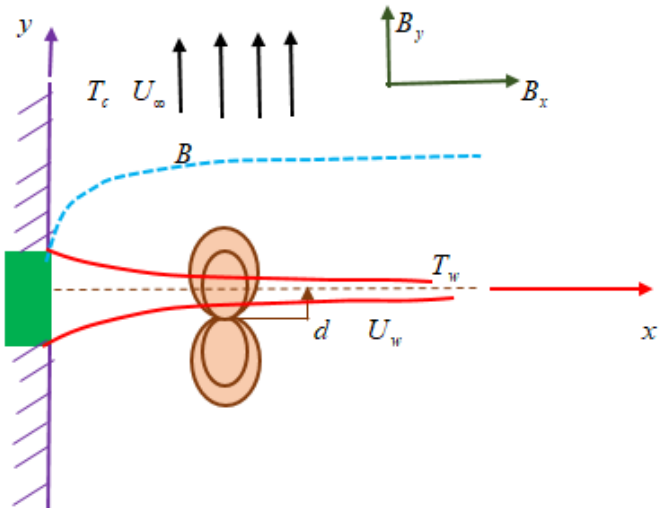

Figure 1: The coordinate system and physical configuration.

The fundamental governing equations could change under the boundary layer approximation to [11, 15, 46]:

$$\frac{\partial u}{\partial x}+\frac{\partial v}{\partial y}=0 \tag{1}$$

$$\rho\left(u\frac{\partial u}{\partial x}+v\frac{\partial u}{\partial y}\right)=-\frac{\partial p}{\partial x}+\mu_0 M\frac{\partial H}{\partial x}-\sigma B_y^2 u+\sigma B_x B_y v+\mu\frac{\partial^2 u}{\partial y^2} \tag{2}$$

$$\rho\left(u\frac{\partial v}{\partial x}+v\frac{\partial v}{\partial y}\right)=-\frac{\partial p}{\partial y}+\mu_0 M\frac{\partial H}{\partial y}-\sigma B_x^2 v+\sigma B_x B_y u+\mu\frac{\partial^2 v}{\partial y^2} \tag{3}$$

$$\rho C_p\left(u\frac{\partial T}{\partial x}+v\frac{\partial T}{\partial y}\right)+\mu_0 T\frac{\partial M}{\partial T}\left(u\frac{\partial H}{\partial x}+v\frac{\partial H}{\partial y}\right)=k\frac{\partial^2 T}{\partial y^2}+q'' \tag{4}$$

The relevant boundary conditions at the sheet $y=A(x+b)^{\frac{1-m}{2}}$ are

$$u(x,y)=U_w=U_0(x+b)^m, v(x,y)=0, T(x,y)=T_w=T_c+D\left(\frac{x+b}{l}\right)^{2m-1} \tag{5}$$

Also, the boundary conditions as $y\to\infty$

$$u(x,y)\to 0, T\to T_c, p+\frac{1}{2}q^2=const \tag{6}$$

where $q=(u,v)$ indicates the dimensional velocity and k,ρ,μ,T,σ,c_p,q'' are stands the blood thermal conductivity, density, viscosity, temperature, electrical conductivity, specific heat, and heat source or sink, respectively. Also, $H=(H_x,H_y)$ denotes strength of magnetic field and magnetic induction is $B(=\mu_0 H)$.

The components of the magnetic force, also known as the Kelvin force, per unit volume are represented by the terms $\mu_0 M\frac{\partial H}{\partial x}$ and $\mu_0 M\frac{\partial H}{\partial y}$ in equations (2) and (3), while the thermal force is represented by the term in equation (4). Moreover, the magnetohydrodynamic $-\sigma B_y^2 u+\sigma B_x B_y v$ and $-\sigma B_x^2 v+\sigma B_x B_y u$, respectively, in equations (2) and (3) reflect the Lorentz force per unit volume in the x and y directions.

In the event of a non-uniform heat source or sink, we can describe the space- and temperature-dependent internal heat generation or absorption using [47-49], with the term q'' appearing on the right-hand side of (4) in the form of

$$q'' = \frac{kU_w(x)}{(x+b)^m \nu}[A^*(T_w - T_c)f' + B^*(T - T_c)], \tag{7}$$

the coefficients A^* and B^* being constants. We shall consider the following two cases: (i) for heat generation $A^* > 0$ and $B^* > 0$and (ii) for heat absorption $A^* < 0$ and $B^* < 0$.

Following [7-8], the change of magnetic field along axial and radial axis is given by:

$$\frac{\partial H}{\partial x} = -\frac{\gamma}{2\pi}\frac{2(x+b)}{(y+d)^4} \text{ and } \frac{\partial H}{\partial y} = \frac{\gamma}{2\pi}\left[-\frac{2}{(y+d)^3} + \frac{4(x+b)^2}{(y+d)^5}\right]$$

The linear equation of magnetization Minvolving$H$ and T, can be written as in [50],

$$M = KH(T_c - T), \tag{8}$$

where K is a constant and T_c is the Curie temperature. This relation was used while analyzing different biomagnetic fluid flow problems [51, 52].

3. Transformation of Equations

To simplify the governing equations, the following similarity variables are used in this study ([34, 37, 39]):

$$\eta = y\sqrt{\frac{m+1}{2}\frac{U_0(x+b)^{m-1}}{\nu}}, m \neq 1 \tag{9}$$

$$\psi(x,y) = f(\eta)\sqrt{\frac{2}{m+1}\nu U_0(x+b)^{m+1}} \tag{10}$$

$$\theta(\eta) = \frac{T - T_c}{T_w - T_c} \tag{11}$$

and

$$P(\eta) = U_0\nu\frac{m+1}{2}\frac{U_0(x+b)^{m+1}}{\nu} \tag{12}$$

Following the definition of $\psi(x,y)$ one can find:

$$u = \frac{\partial \psi}{\partial y} = U_0(x+b)^m f'(\eta) = U_w f'(\eta)$$

and

$$v = -\frac{\partial \psi}{\partial x} = -\sqrt{\nu\frac{m+1}{2}U_0(x+b)^{m-1}}\left(f(\eta) + \eta\frac{m-1}{m+1}f'(\eta)\right)$$

Substituting equations (9)-(12), into equations (2)-(4), the similarity equations become

$$f''' + ff'' - \frac{2m}{m+1}f'^2 + \frac{(m+1)^2}{2}p - (m+1)\frac{\delta^2\beta\theta}{(\eta+\delta)^6} - M_n f' = 0 \tag{13}$$

$$p' + \frac{6\delta^2\beta\Theta}{(\eta+\delta)^7} = 0 \tag{14}$$

$$\Theta'' - P_r\left[\frac{2(2m-1)}{m+1}f'\Theta - f\Theta'\right] + \frac{2\delta^2\lambda\beta(\Theta - \varepsilon)}{(\eta+\delta)^5}f + A^*f' + B^*\Theta = 0 \tag{15}$$

associate boundary conditions:

$$f(0)=\alpha\left(\frac{1-m}{1+m}\right), f'(0)=1, f'(\infty)\to 0, \theta(0)=1, \theta(\infty)\to 0. and p(\infty)\to 0 \quad (16)$$

where$\alpha = A\sqrt{\frac{m+1}{2}\frac{U_0}{\nu}}$ is the thickness wall parameter, and $\alpha=\eta$ represents the surface of the plate.

In the sequel, we shall consider the following dimensionless parameter Prandtl number $P_r=\frac{\mu C_p}{k}$, Magnetohydrodynamic interaction parameter $M_n=\frac{\sigma\mu_0^2 H}{U_0\rho}$, Viscous dissipation parameter $\lambda=\frac{U_0\mu^2}{\rho k(T_c-T_w)}$, Ferromagnetic number $\beta=\frac{\gamma}{2\pi}\frac{\mu_0 KH(0,0)(T_c-T_w)\rho}{\mu^2}$, Temperature parameter $\varepsilon=\frac{T_w}{T_c-T_w}$, distance $\delta=\left(\frac{U_0\rho}{\mu}\right)^{\frac{1}{2}}d$.

We shall also examine physical quantities, coefficient of skin friction and the local Nusselt number which is denoted by $C_{fx}$and N_u respectively and defined by

$$C_{fx}=-2\sqrt{\frac{m+1}{2}}R_e^{-\frac{1}{2}}f''(0) \text{ and } N_u=-\sqrt{\frac{m+1}{2}}R_e^{-\frac{1}{2}}\theta'(0),$$

where $R_e=\frac{u_w(x+b)}{\nu}$ is the local Reynolds numbers.

4. Numerical Method

The computational accomplishment of the nonlinear differential equations (13) to (15) with (16) are obtained using an approximate technique with central difference technique, tridiagonal maxtrix and iterative procedure. This methodology is described in [53, 54] has also been elongated, applied and affirmed in [8, 9]. For this method, it is indispensable to select an arbitrary finite value of n_∞ and arbitrary step size $h=0.01$ has been used to attain the numerical solution with n_∞. After this an appropriate value n_∞ as $(y\to\infty)$ need to be ascertained. For the convergence criteria, we take the different initial guess. This system is repeated until the corrected result obtained up to a desired accuracy. By trial and error, we fixed $n_\infty=8$ and set the value of the tolerance is $\varepsilon=10^{-4}$.

4.1. Assignment of the Parameter Values

Since blood is our base fluid in this study, therefore we consider the following physical properties from the study [15, 55-56] as$\rho=1050kg/m^3$, $\mu=3.2\times10^{-3}kgm^{-1}s^{-1}$, $\sigma=0.8sm^{-1}$, $c_p=3.9\times10^3Jkg^{-1}k^{-1}$ and $k=0.5Jm^{-1}s^{-1}k^{-1}$. Considering these one can find the adjustable Prandtl number for human blood is 25, viscous dissipation number is 6.4×10^{-14}. Additionally, consider blood temperature and plate temperature respectively are as $T_c=41^0C$, and $T_w=37^0C$. Which gives the value $\varepsilon=78.5$. Table **1** presents the assigned physical parameter values that handled in numerical approach.

Table 1: Values of estimated parameters in computational process.

Parameter	Estimated Values	References
β	0, 2, 4, 5, 6, 8, 10	[52, 57, 58]
M_n	0, 1, 2, 3, 4, 5, 10	[23, 59-60]
α	0, 0.25, 0.5, 1, 1.5	[34, 37, 39]
m	0.1, 0.5, 2, 3	[34, 37, 39]
A^*	-0.6, 0, 0.6	[47-49]
B^*	-0.6, 0, 0.6	[47-49]

5. Results and Discussion

We go over how the governing parameters such as $m, \alpha, \beta, M_n, A^*, B^*$ affect the blood flow's temperature, pressure, and velocity distributions. The graph in Figs. (**2**-**18**) is used to discuss the computational results.

When β = 0, Mn = 0, α = 0.5, 0.25, and the current study are compared with those of Fang *et al*. [34] and Kader *et al*. [37] in Table **2**, sufficient accuracy is found.

Table 2: Comparison of $-f''(0)$ for different values of α and m.

α	m	Fang *et al*. [34]	Kader *et al*. [37]	Present Analysis $-f''(0)$
0.5	10	1.0603	1.0602	1.0602
	9	1.0589	1.0589	1.0590
	7	1.0550	1.0550	1.0557
	5	1.0486	1.0486	1.0503
	3	1.0359	1.0358	1.0397
	2	1.0234	1.0235	1.0295
	-0.5	1.1667	1.1667	1.1647
0.25	10	1.1434	1.1434	1.1432
	9	1.1405	1.1405	1.1404
	7	1.1326	1.1326	1.1327
	5	1.1186	1.1186	1.1198
	3	1.0905	1.0905	1.0933

We first examine the effect of the thickness parameter (α) on the velocity, temperature, and pressure distributions in the case of β = 10 and Mn = 5. The calculated values are displayed, correspondingly, in Figs. (**2**-**4**).

Fig. (**2**) reveals that for $f'(\eta)$ with power index$m = 0.1$, the $\boldsymbol{f'(\eta)}$ at any point in the vicinity of the plate reduces with gradually increase in the thickness parameter (α). However, when $\mathrm{m} = 2$, the trend is reversed. Fig. (**3a-3b**) reveals the blood $\theta(\eta)$ distribution for $m = 0.1$, and $m = 2$ respectively. One may observe that when $m = 0.1$, with gradual increase in the thickness parameter ($\boldsymbol{\alpha}$), the temperature decreases, but for $m = 2$ an opposite behavior is noticed.

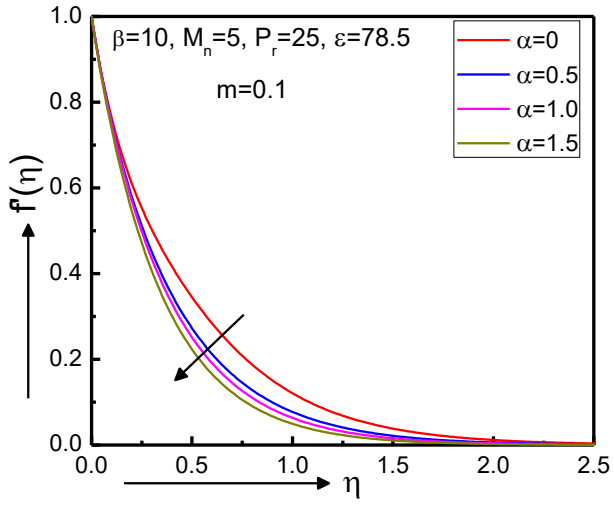

Figure 2: (a) Behavior of α on $f'(\eta)$ with $m = 0.1$.

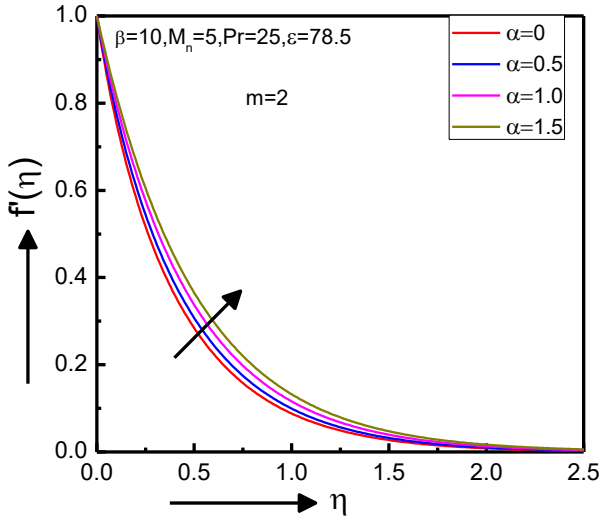

Figure 2: (b) Behavior of α on $f'(\eta)$ with $m = 2$.

Fig. (**4**) express the variation of the pressure distribution P with various values of $m = 0.1$ and $m = 2$. From this figure, we observed that the pressure distribution P reduces with α increases for $m = 0.1$ but the observation is reverse for $m = 2$. It may further observed that the values of $\boldsymbol{P(\eta)}$ close to the wall whenever $m = 2$ than the corresponding values computed for $m = 0.1$. Figs. (**5-7**) express the effects of m on the $f'(\eta), \theta(\eta)$ and $P(\eta)$ distributions for a fixed value of α=0.5. From this figure, we see that as the value of m increases, all the three physical variables increase.

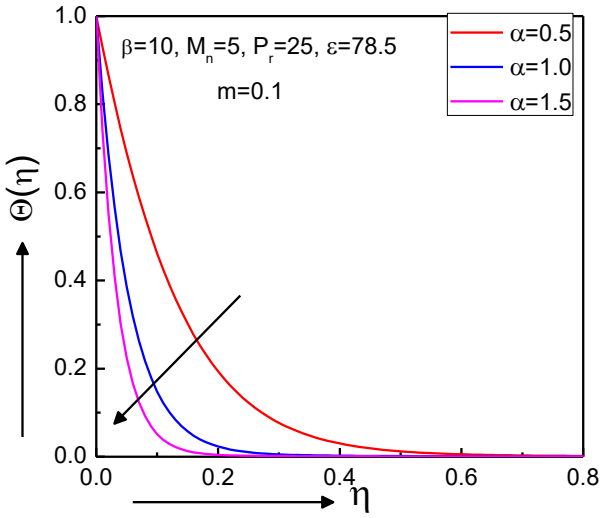

Figure 3: (a) Behavior of α on $\theta(\eta)$ with $m = 0.1$.

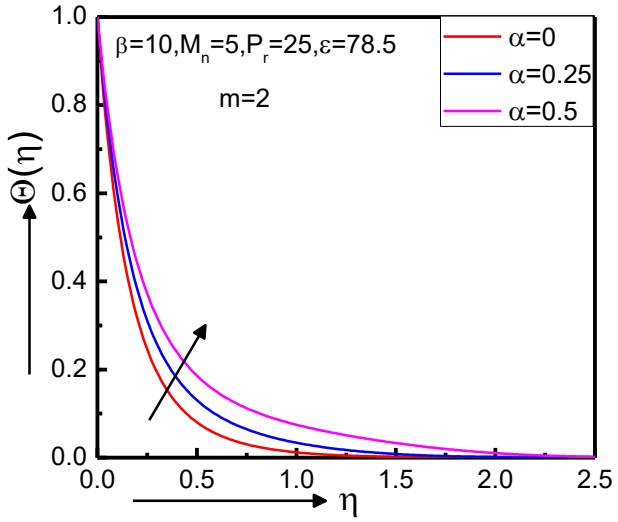

Figure 3: (b) Behavior of α on $\theta(\eta)$ with $m = 2$.

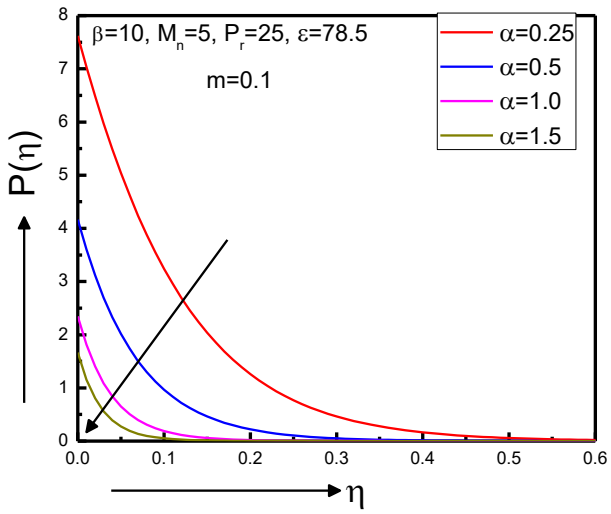

Figure 4: (a) Behavior of α on $P(\eta)$ with $m = 0.1$.

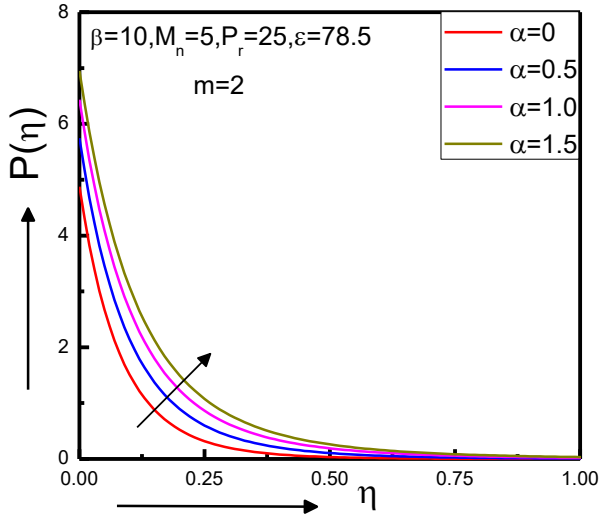

Figure 4: (b) Behavior of α on $P(\eta)$ with $m = 2$.

Figs. (**8-9**) depict the effects of A^* andB^* on $\theta(\eta)$ distributions respectively. It is noticed that the increases of heat source parameter (A^*) results in increase of temperature profile for B*=0.6 and a similar behavior is observed when $A^* = 0.6$ and B^* increases.

Figs. (**10-12**) depict the effects of M_n on $f'(\eta)$, $\theta(\eta)$ and $P(\eta)$. Fig. (**10**) shows that $f'(\eta)$ is significantly reduced as M_n rise due to induced Lorentz force in the flow field. Therefore, it can be said that the temperature field's anticipated behavior is not qualitatively changed by the induced magnetic field.

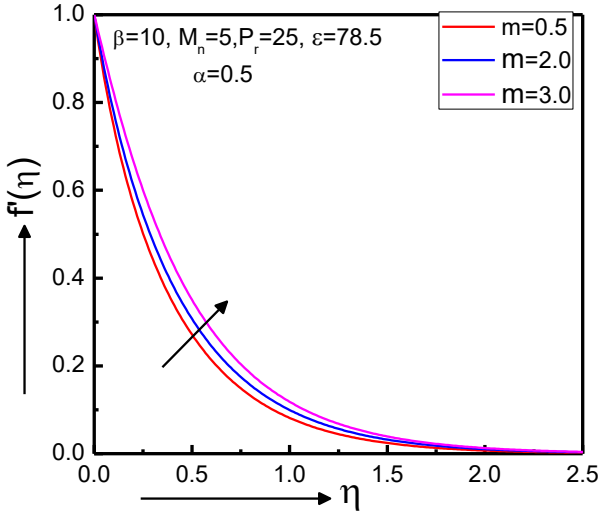

Figure 5: Behavior of m on $f'(\eta)$.

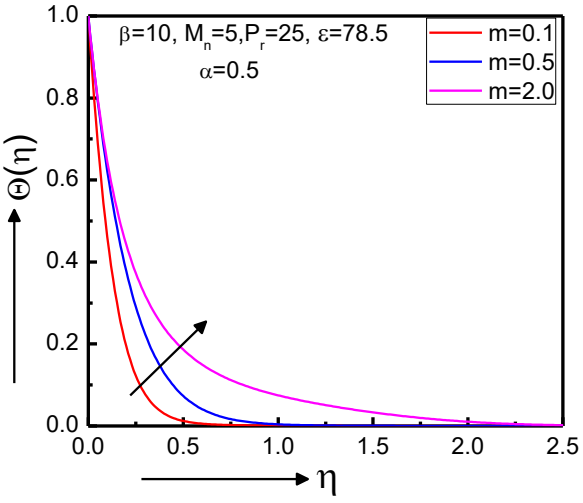

Figure 6: Behavior of m on $\theta(\eta)$.

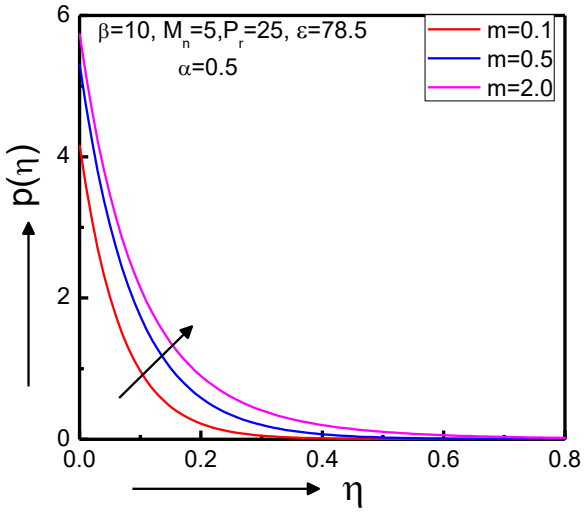

Figure 7: Behavior of m on $P(\eta)$.

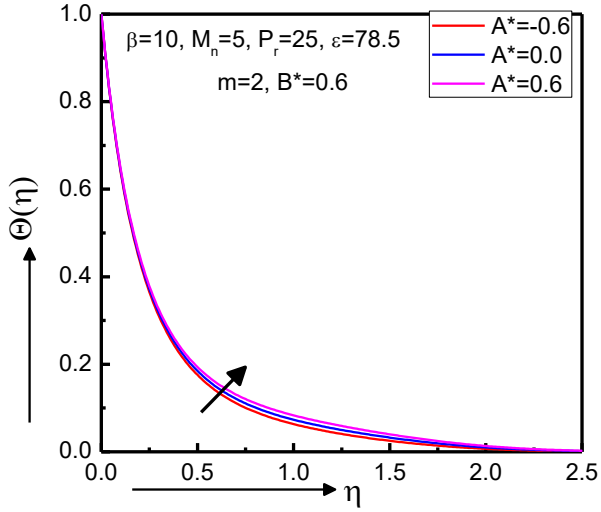

Figure 8: Behavior of $A*$ on $\theta(\eta)$.

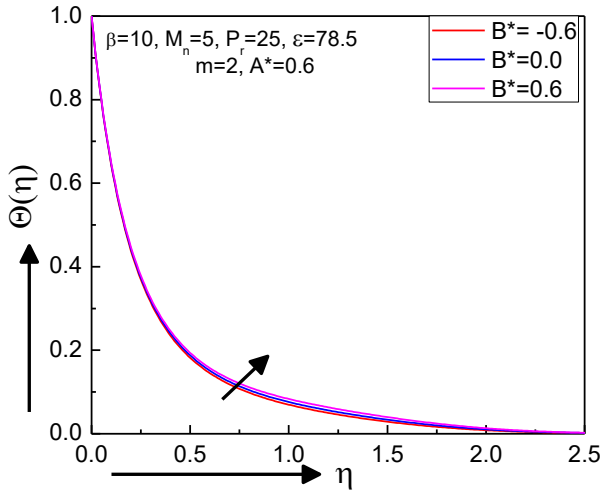

Figure 9: Behavior of $B*$ on $\theta(\eta)$.

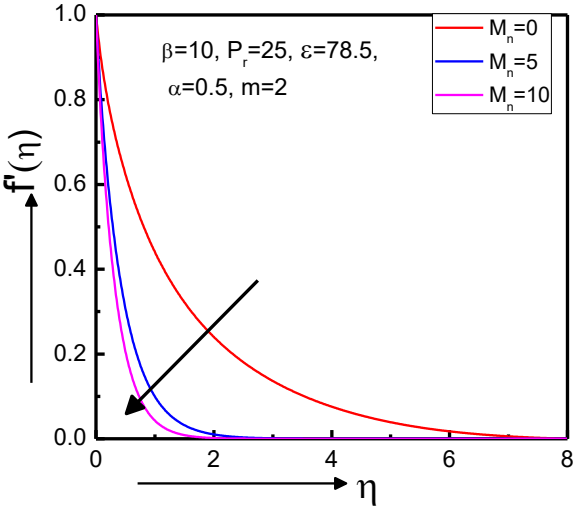

Figure 10: Behavior of M_n on $f'(\eta)$.

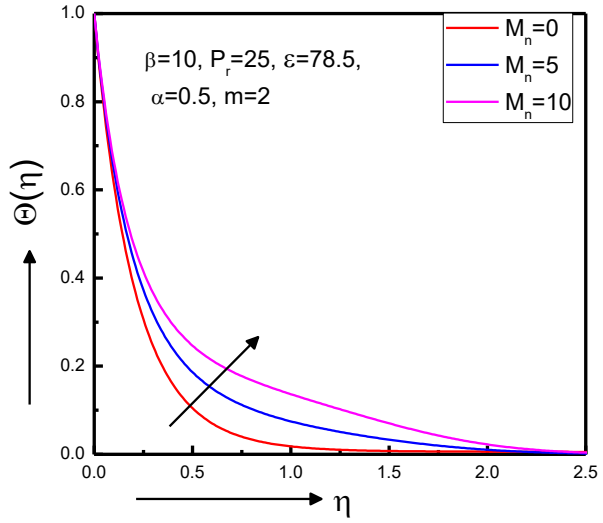

Figure 11: Behavior of M_n on $\theta(\eta)$.

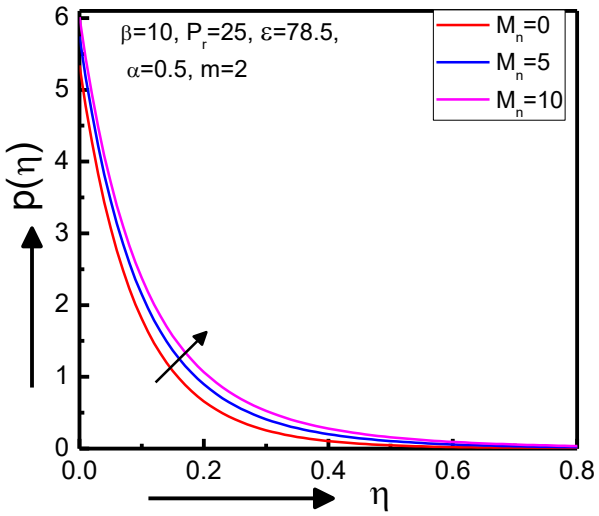

Figure 12: Behavior of M_n on $P(\eta)$.

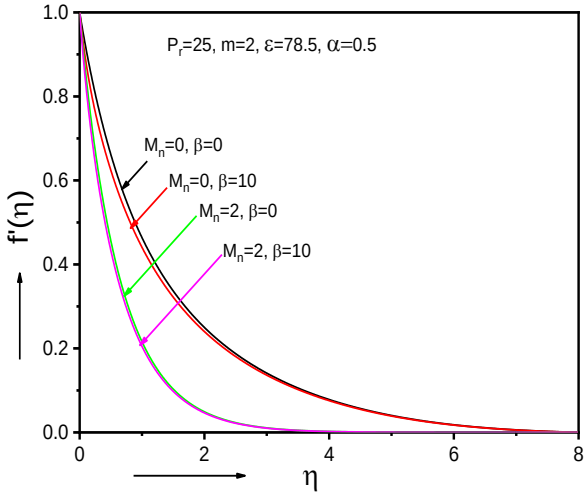

Figure 13: Behavior of $M_n$and β on $f'(\eta)$.

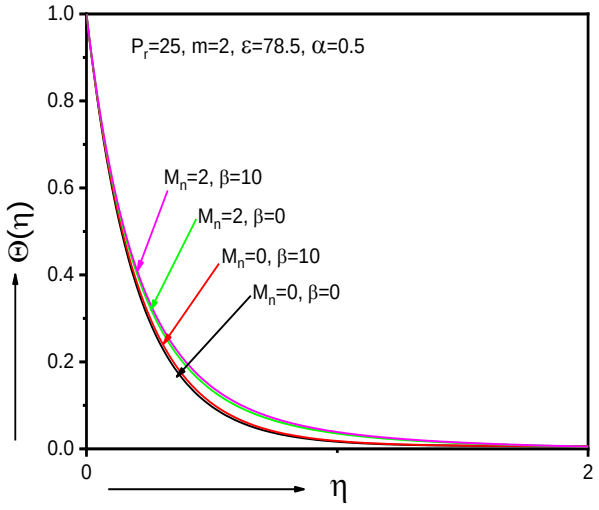

Figure 14: Behavior of $M_n$and β on $\theta(\eta)$.

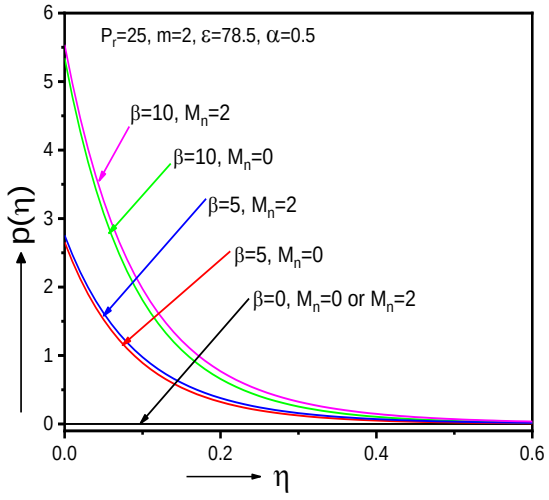

Figure 15: Behavior of $M_n$and β on $P(\eta)$.

Figs. (**13**-**15**) exhibit the nature of $f'(\eta)$,$P(\eta)$ and $\theta(\eta)$ distributions respectively. The curves have been plotted for $(\beta = 0, M_n = 0)$, $(\beta \neq 0, M_n = 0)$, $(\beta = 0, \mathrm{M_n} \neq 0)$ and $(\beta \neq 0, \mathrm{M_n} \neq 0)$. It is noticed that $f'(\eta)$ is diminished, when either β or M_n increases. It is noted that the major impact on $f'(\eta)$ is observed, when M_n increases. This has also been revealed in Fig. (**10**). From this observation we concluded that the impact of β on $f'(\eta)$ is much less than that of M_n. But for $\theta(\eta)$ and $P(\eta)$ distributions are considerably affected due to changes in both β and M_n.

The impact of both β and M_n on the important physical variables skin friction, local heat transfer rate and wall pressure is well illustrated in Figs. (**16**-**18**). Fig. (**16**) express that the local skin friction coefficient $(f''(0))$ changes in a rectilinear manner as β increases for all values of M_n examined here (Fig. **16a**). However, Fig. (**16b**) shows that for fixed values of β, the variation of wall shear with M_n is curvilinear. Fig. (**16c-16d**) display the variation of the wall shear versus m for several values of β. It is important to observe that these variations are highly nonlinear.

Fig. (**16c**) shows that the wall shear parameter increases asβ grows when $0 < m < 7$, but when m > 7, the reverse tendency is observed. It is important to observe that the dimensionless wall shear parameter reaches its maximum at $m \approx 3$for a certain value of m as B1 grows. The application of the magnetization and polarization effects has no influence on the wall shear parameter value for $m = 7$. Fig. (**16d**) shows that the pattern is reversed as the value of $m \approx 3$ grows, indicating that when $m \cong 3$, the wall shear parameter increases as M_n increases.

The rate of heat transfer at the sheet is usually defined by the ratio $\Theta * (0) = \frac{\Theta\prime(0)}{\Theta\prime(0)|\beta=M_n=0}$. The variations of $\Theta^*(0)$ with β and M_n are presented in Fig. (**17a-17b**). Fig. (**17a**) shows that with increase in β, $\Theta^*(0)$ reduces linearly, while Fig. (**17b**) shows that $\Theta^*(0)$ decreases in a nonlinear manner, when M_n increases. The changes of the wall pressure $\mathrm{P}(0)$ presented in Fig. **18** with β is found shows that the to be a monotonically increasing with gradually increase of the ferromahnetic parameter β. From this discovery, it is interesting to note that $f''(0)$, $\Theta^*(0)$, and $P(0)$ vary nonlinearly with the M_n and m but linearly with β throughout the sheet.

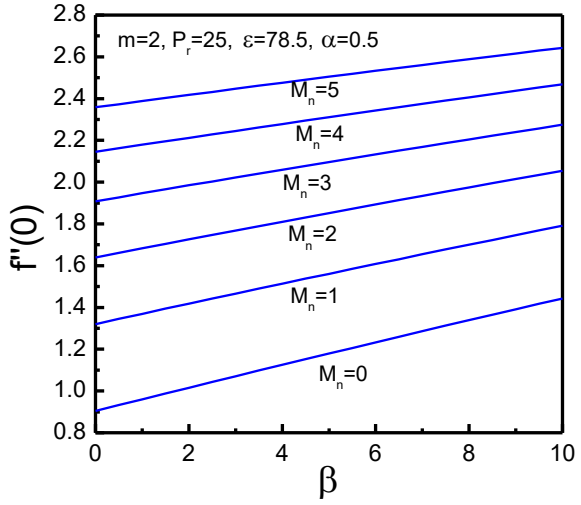

Figure 16: (**a**) Profile of wall share parameter versus β for several values ofM_n.

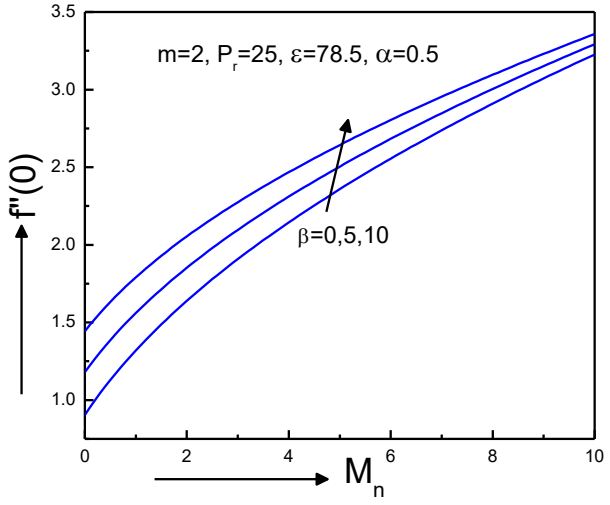

Figure 16: (**b**) Profile of wall share parameter versus M_n for several values of β.

6. Conclusions

This work examined the blood flow and heat performance over a nonlinear stretching sheet with variable thickness under the interplay of MHD and FHD in addition to a nonlinear heat source and sink. The finite difference method, an effective computational technique, was used to produce the computational results. Taking into account the geometry of magnetic dipoles, the present study aims to improve and clarify the analysis of the stretchable variable thickness sheet in nonlinear form. From the current study, the following conclusions can be drawn:

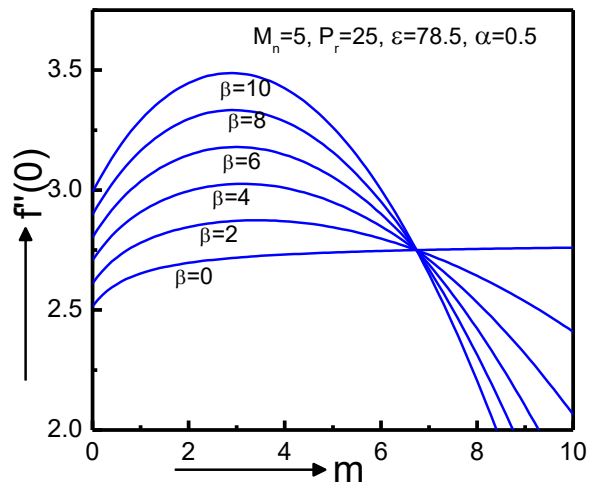

Figure 16: (c) Profile of wall share parameter versus m for several values of β.

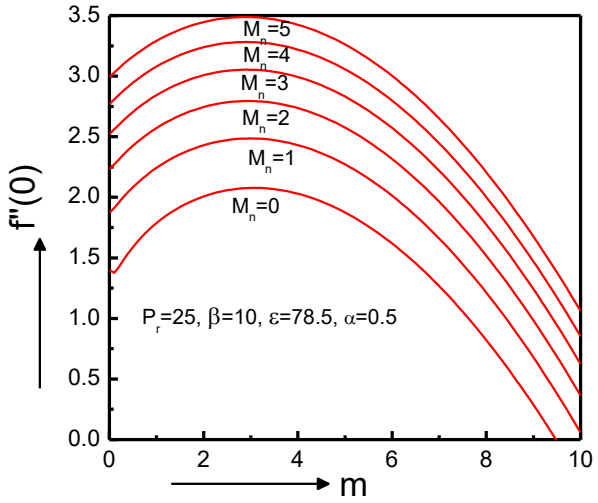

Figure 16: (d) Profile of wall share parameter versus m for several values of M_n.

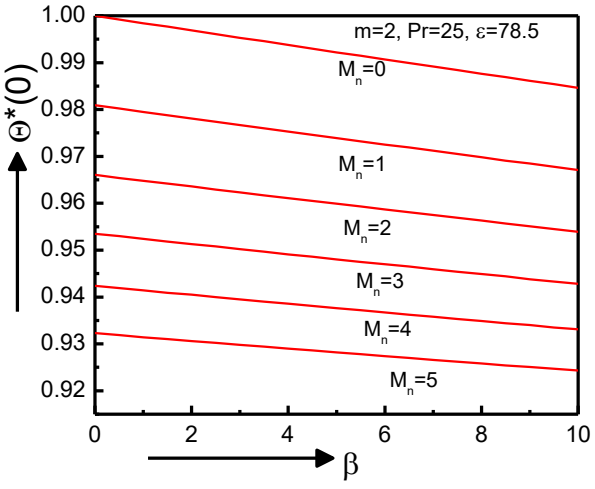

Figure 17: (a) Profile of wall heat transfer parameter versus β for several values of M_n.

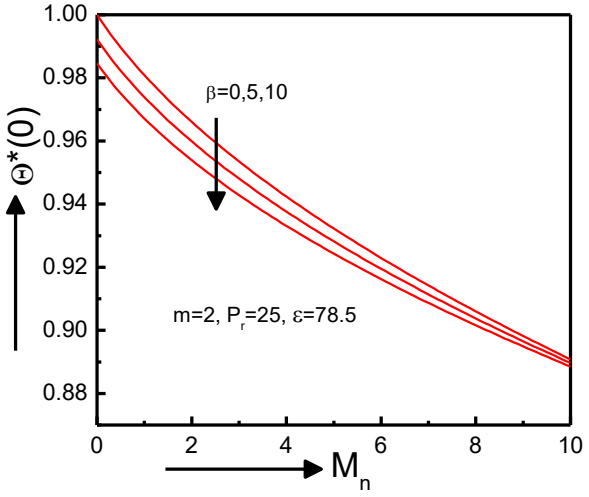

Figure 17: (b) Profile of wall share parameter versus M_n for several values of β.

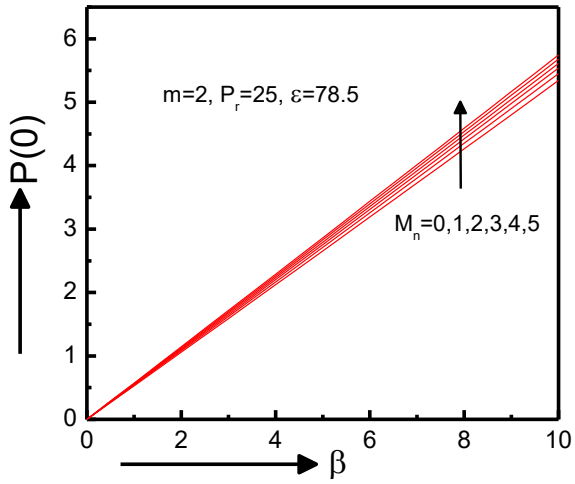

Figure 18: Profile of wall pressure parameter versus β for several values of M_n.

(i) Blood pressure and temperature attain highest in BFD cases when compared to MHD and/or FHD instances; the velocity profile shows an opposite tendency.

(ii) The blood velocity, temperature and pressure profiles in boundary layer diminishes for α when the values of m is small but improved significantly in case of greater m.

(iii) Blood temperature and pressure in the flow field enhanced with the parameter m, A^*, B^*, M_n.

(iv) The velocity distribution rises with m but reduces for M_n.

(v) The skin friction coefficient boost up for the values of M_n, β but reverse phenomena is observed in the rate of heat transfer and wall pressure distributions.

Nomenclature

η	Dimensionless co-ordinate	m	Power law index parameter
θ	Dimensionless temperature	b	Constant stretching rate factor
U_w	Stretching velocity [ms^{-1}]	μ	Dynamic viscosity in [$Kgm^{-1}s^{-1}$]
U_∞	Free stream velocity [ms^{-1}]	μ_0	Magnetic fluid permeability in [NA^{-2}]
U_0	Constant velocity [ms^{-1}]	C_p	Specific heat at constant Pressure [$JKg^{-1}K^{-1}$]
T	Fluid temperature [K]	ρ	Fluid density [$Kg^{-1}m^{-3}$]
T_w	Surface temperature [K]	υ	Kinematic viscosity in [m^2s^{-1}]
T_c	Curie temperature [K]	σ	Electrical conductivity in [Sm^{-1}]
d	Distance [m]	ε	Temperature parameter
B	Magnetic induction [Am^{-1}]	k	Thermal conductivity [$Jm^{-1}s^{-1}K^{-1}$]
β	Ferromagnetic interaction parameter	H	Magnetic field intensity [Am^{-1}]
M_n	Magnetic field parameter	α	Wall thickness parameter
Pr	Prandtl number	M	Magnetization [Am^{-1}]

Conflict of Interest

The authors declare no conflict of interest.

Funding

J.C. Misra, would like to thank the Department of Science and Technology, SERB, Government of India, for approving Research Project No. CRG/2018/000158.

References

[1] Haik Y, Pai V, Chen CJ. Development of magnetic device for cell separation. J Magn Magn Mater. 1999; 194: 254-61. https://doi.org/10.1016/S0304-8853(98)00559-9

[2] Voltaira PA, Fotiadis DI, Michalis LK. Hydrodynamics of magnetic drug targeting. J Biomech. 2002; 35: 813-21. https://doi.org/10.1016/S0021-9290(02)00034-9

[3] Ruuge EK, Rusetski AN. Magnetic fluid as drug carries: targeted transport of drugs by a magnetic field. J Magn Magn Mater. 1993; 122: 335-9. https://doi.org/10.1016/0304-8853(93)91104-F

[4] Misra JC, Shit GC. Flow of a biomagnetic viscoelastic fluid in a channel with stretching walls. J Appl Mech. 2009; 76: 1-9. https://doi.org/10.1115/1.3130448

[5] Misra JC, Shit GC. Biomagnetic viscoelastic fluid flow over a stretching sheet. Appl Math Comput. 2009; 210: 350-61. https://doi.org/10.1016/j.amc.2008.12.088

[6] Misra JC, Sinha A, Shit GC. Flow of a biomagnetic viscoelastic fluid: application to estimation of blood flow in arteries during electromagnetic hyperthermia, a therapeutic procedure for cancer treatment. Appl Math Mech. 2011; 13: 1405-20. https://doi.org/10.1007/s10483-010-1371-6

[7] Andersson HI, Valnes OA. Flow of a heated ferrofluid over a stretching sheet in the presence of a magnetic dipole. Acta Mechanica. 1998; 128: 39-47. https://doi.org/10.1007/BF01463158

[8] Tzirtzilakis EE, Kafoussias NG. Biomagnetic fluid flow over a stretching sheet with nonlinear temperature dependent magnetization. Z Angew Math Phys. 2003; 54: 551-65. https://doi.org/10.1007/s00033-003-1100-5

[9] Tzirtzilakis EE, Tanoudis GB. Numerical study of biomagnetic fluid flow over a stretching sheet with heat transfer. Int J Num Methods Heat Fluid Flow. 2003; 13: 830-48. https://doi.org/10.1108/09615530310502055

[10] Higashi T, Yamagishi A, Takeuchi T, Kawaguchi N, Sagawa S, Onishi S, *et al*. Orientation of erythrocytes in a strong static magnetic field. J Blood. 1993; 82: 1328. https://doi.org/10.1182/blood.V82.4.1328.1328

[11] Haik Y, Pai V, Chen CJ. Biomagnetic fluid dynamics, In: Shyy W, Narayanan R, Eds., Fluid dynamics at interfaces. Cambridge University Press; 1999, pp. 439-52.

[12] Rosensweig RE. Magnetic fluids. Ann Rev Fluid Mech. 1987; 19: 437-61. https://doi.org/10.1146/annurev.fl.19.010187.002253

[13] Rosensweig RE. Ferrohydrodynamics. Cambridge University Press; 1985.

[14] Bashtovoy VG, Berkovsky BM, Vislovich AN. Introduction to Thermomechanics of magnetic fluids. Heidelberg: Spinger-Verlag, Berlin; 1988.

[15] Tzirtzilakis EE. A Mathematical model for blood flow in magnetic field. Phys Fluids. 2005; 17: 077103-1-14. https://doi.org/10.1063/1.1978807

[16] Ramamurthy G, Shanker B. Magnetohydrodynamic effects on blood flow through porous channel. Med Biol Eng Comput. 1994; 32: 655-9. https://doi.org/10.1007/BF02524242

[17] Rusli N, Beng Hong A, Kasima EH, Yassin AYM, Amin N. Numerical computation of a two-dimensional biomagnetic channel flow. Int J Mod Phys. 2012; 9: 178-92. https://doi.org/10.1142/S2010194512005247

[18] Tzirtzilakis EE, Xenos M, Loukopolos VC, Kafoussias NG. Turbulent biomagnetic fluid flow in a rectangular channel under the action of localized magnetic field. Int J Eng Sci. 2006; 44: 1205-24. https://doi.org/10.1016/j.ijengsci.2006.07.005

[19] Misra JC, Sinha A. Effect of thermal radiation on MHD flow of blood and heat transfer in a permeable capillary in stretching motion. Heat Mass Transfer. 2013; 9: 617-28. https://doi.org/10.1007/s00231-012-1107-6

[20] Pavlov KB. Magnetohydrodynamic flow of an incompressible viscous fluid caused by deformation of a plane surface. Magnitnaya Gidrodinamika. 1974; 10: 146-8. http://doi.org/10.22364/mhd

[21] Andersson HI. An exact solution of the Navier-Stokes equations for magnetohydrodynamic flow. Acta Mechanica. 1995; 113: 241-4. https://doi.org/10.1007/BF01212646

[22] Andersson HI. Slip flow past a stretching surface. Acta Mechanica. 2002; 158: 121-5. https://doi.org/10.1007/BF01463174

[23] Loke YY, Merkin JH, Pop I. MHD oblique stagnation point flow towards a stretching / shrinking surface. Mechanica. 2015; 50: 2949-61. https://doi.org/10.1007/s11012-015-0188-y

[24] Dulal P, Gopinath M. MHD convective stagnation point flow of nanofluids over a non-isothermal stretching sheet with induced magnetic field. Mechanica. 2015; 50: 2023-35.

[25] Ishak A, Nazar R, Pop I. Mixed convection boundary layers in the stagnation point flow towards a stretching vertical sheet. Meccanica. 2006; 41: 509-18. https://doi.org/10.1007/s11012-006-0009-4

[26] Ishak A, Jafar K, Nazar R, Pop I. MHD stagnation point flow towards a stretching sheet. Physica A. 2009; 388: 3377-83. https://doi.org/10.1016/j.physa.2009.05.026

[27] Ishak A, Bachok N, Nazar R, Pop I. MHD mixed convection flow near the stragnation point on a vertical permeable surface. Physica A. 2010; 389: 40-6. https://doi.org/10.1016/j.physa.2009.09.008

[28] Andersson HI. MDH flow of a viscoelastic fluid past a stretching surface. Acta Mechanica. 1992; 95: 227-30. https://doi.org/10.1007/BF01170814

[29] El-Mistikawy MA. MHD flow due to a linearly stretching sheet with induced magnetic field. Acta Mechanica. 2016; 227: 3049-53. https://doi.org/10.1007/s00707-016-1643-0

[30] Ali FM, Nazar R, Arifin NM, Pop I. MHD boundary layer flow and heat transfer over a stretching sheet with induced magnetic field. Heat Mass Transfer. 2011; 47: 155- 62. https://doi.org/10.1007/s00231-010-0693-4

[31] Ali FM, Nazar R, Arifin NM, Pop I. MHD mixed convective boundary layer flow towards a stagnation point flow on a vertical surface with induced magnetic field. ASME J Heat Transfer. 2011; 133: 022502-1. https://doi.org/10.1115/1.4002602

[32] Pop I, TY Na. A note on MHD flow over a stretching permeable surface. Mech Res Comm. 1998; 25: 263-9. https://doi.org/10.1016/S0093-6413(98)00037-8

[33] Devi SPA, Thiyagarajan M. Steady nonlinear hydromag- netic flow and heat transfer over a stretching surface of variable temperature. Heat Mass Transfer. 2006; 42: 671-7. https://doi.org/10.1007/s00231-005-0640-y

[34] Fang T, Zhang J, Zhong Y. Boundary layer flow over a stretching sheet with variable thickness. Appl Math Comput. 2012; 218: 7241-52. https://doi.org/10.1016/j.amc.2011.12.094

[35] Lee LL. Boundary layer over a thin needle. Phys Fluid. 1967; 10: 822-8. https://doi.org/10.1063/1.1762194

[36] Ishak A, Nazar R, Pop I. Boundary layer flow over a continuously moving thin needle in a parallel free stream. Chinese Phys Lett. 2007; 24: 2895-7. https://doi.org/10.1088/0256-307X/24/10/051

[37] Khader MM, Megahed AM. Approximate solutions for the flow and heat transfer due to a stretching sheet embedded in a porous medium with variable thickness, variable thermal conductivity and thermal radiation using Laguerre collocation method. Appl Appl Math. 2015; 10: 817-34.

[38] Prasad KV, Vajravelu K, Hanumesh V. MHD casson nanofluid flow and heat transfer at a stretching sheet with variable thickness. J Nanofluids. 2016; 5: 1-13. https://doi.org/10.1166/jon.2016.1228

[39] Vajravelu K, Ronald L, Dewasurendra M, Prasad KV. Mixed convective boundary layer MHD flow along a vertical elastic sheet. Int J Appl Comput Math. 2017; 3: 2501-18. https://doi.org/10.1007/s40819-016-0252-x

[40] Rashed AS, Mabrouk SM, Wazwaz AM. Unsteady three-dimensional laminar flow over a submerged plate in electrically conducting fluid with applied magnetic field. Waves Random Complex Media. 2023; 33: 505-24. https://doi.org/10.1080/17455030.2021.1883147

[41] Rashed AS, Mahmoud TA, Kassem MM. Behavior of nanofluid with variable brownian and thermal diffusion coefficients adjacent to a moving vertical plate. J Appl Comput Mech. 2021; 7: 1466-79. https://doi.org/10.22055/JACM.2021.34852.2483

[42] Rashed AS, Mahmoud TA, Kassem MM. Analysis of homogeneous steady state nanofluid surrounding cylindrical solid pipes. Egypt Int J Eng Sci Tchnol. 2020; 31: 71-82. https://doi.org/10.21608/EIJEST.2020.38518.1003

[43] Rashed AS, Nasr EH, Kassem MM. Boundary Layer Analysis Adjacent to Moving Heated Plate Inside Electrically Conducting Fluid with Heat Source/Sink. Int J Heat Technol. 2020; 38: 682-8. https://doi.org/10.18280/ijht.380312

[44] Qi X, Zhang H, Sun X, Wang Z. Numerical investigation on flow-field characteristics towards removal of free-water by a separator with coalescing plates. J Adv App Comput Math. 2023; 10: 1-17. https://doi.org/10.15377/2409-5761.2023.10.1

[45] Wang Z, Qi X, Zhuang Y, Wang Q, Sun X. Effect of flow field and electric field coupling on oil–water emulsion separation. Desalin Water Treat. 2023; 283: 79-6.

[46] Tzirtzilakis EE, Xenos MA. Biomagnetic fluid flow in a driven cavity. Meccanica. 2013; 48: 187-200. https://doi.org/10.1007/s11012-012-9593-7

[47] Abel MS, Mahesha N. Heat transfer in MHD viscoelastic fluid flow over a stretching sheet with variable thermal conductivity, non-uniform heat source and radiation. Appl Math Model. 2008; 32: 1965-83. https://doi.org/10.1016/j.apm.2007.06.038

[48] Raju CSK, Sandeep N, Babu MJ, Sugunamma V. Dual solution for three dimensional MHD flow of a nanofluid over a nonlinearly permeable stretching sheet. Alexandria Eng J. 2016; 55: 151-62. https://doi.org/10.1016/j.aej.2015.12.017

[49] Abel MS, Siddheshwar PG, Nandeppanavar MM. Heat transfer in a viscoelastic boundary layer flow over a stretching sheet with viscous dissipation and non-uniform heat source. Int J Heat Mass Transfer. 2007; 50: 960-6. https://doi.org/10.1016/j.ijheatmasstransfer.2006.08.010

[50] Matsuki H, Yamasawa K, Murakami K. Experimental considerations on a new automatic cooling device using temperature sensitive magnetic fluid. IEEE Trans Magn. 1977; 13: 1143-5. 10.1109/TMAG.1977.1059679

[51] Tzirtzilakis EE. Biomagnetic fluid flow in an aneurysm using ferrohydynamics principles. Phys Fluids. 2015; 27: 061902. https://doi.org/10.1063/1.4922757

[52] Tzirtzilakis EE. Biomagnetic fluid flow in a channel with stenosis. Physica D. 2008; 237: 66-81. https://doi.org/10.1016/j.physd.2007.08.006

[53] Kafoussias NG, Williams EW. An improved approximation technique to obtain numerical solution of a class of two-point boundary value similarity problems in fluid mechanics. Int J Numer Methods Fluid. 1993; 17: 145-62. https://doi.org/10.1002/fld.1650170204

[54] Kafoussias NG, Williams EW. Thermal-diffusion and diffusion-thermo effects on mixed free forced convective and mass transfer boundary layer flow with temperature dependent viscosity. Int J Eng Sci. 1995; 33: 1369-84. https://doi.org/10.1016/0020-7225(94)00132-4

[55] Alam J, Murtaza MG, Tzirtzilakis, EE, Ferdows. Parametric simulation of Biomagnetic fluid with magnetic particles over a swirling stretchable cylinder under magnetic field effet. BioNanoSci. 2023; 13: 929-46. https://doi.org/10.1007/s12668-023-01117-x

[56] Ferdows M, Alam J, Murtaza MG, Tzirtzilakis, EE. Effects of magnetic particles diameter and particles spacing on Biomagnetic flow and heat transfer over a linear/non-linear stretched cylinder in the presence of magnetic dipole. J Mech Med Biol. 2023; 23: 2350036. https://doi.org/10.1142/S0219519423500367

[57] Tzirtzilakis EE. A simple numerical methodology for BFD problems using stream function vorticity formulation. Comput Numer Methods Eng. 2008; 24: 683-700. https://doi.org/10.1002/cnm.981

[58] Murtaza MG, Alam J, Tzirtzilakis EE, Ferdows M. Numerical simulation of slip flow and heat transfer of biomagnetic fluid over a stretching sheet in the presence of a magnetic dipole with temperature dependent viscosity. Contemp Math. 2023; 4: 345-59. https://doi.org/10.37256/cm.4220232685

[59] Alam J, Murtaza MG, Tzirtzilakis, EE, Ferdows M. Magnetohydrodynamic and Ferrohydrodynamic interactions on the biomagnetic flow and heat transfer containing magnetic particles along a stretched cylinder. Eur J Comput Mech. 2022; 31:1-40. 10.13052/ejcm2642-2085.3111

[60] Alam J, Murtaza MG, Tzirtzilakis EE, Ferdows M. A parametric simulation of MHD flow and heat transfer of blood-Fe_3O_4 over an exponentially stretching cylinder. BioNanoSci. 2023; 13: 891-9. https://doi.org/10.1007/s12668-023-01141-x